

Measuring and interpreting CO₂ fluxes at regional scale: the case of the Apennines, Italy



Francesco Frondini¹, Carlo Cardellini^{1,2}, Stefano Caliro³, Giulio Beddini¹, Angelo Rosiello¹ & Giovanni Chiodini^{2*}



¹ Dipartimento di Fisica e Geologia, Università degli Studi di Perugia, Via Pascoli snc, 06123 Perugia, Italy

² Istituto Nazionale di Geofisica e Vulcanologia, Sezione di Bologna, Via Creti 12, 40128 Bologna, Italy

³ Istituto Nazionale di Geofisica e Vulcanologia, Osservatorio Vesuviano, Via Diocleziano 328, 80124 Napoli, Italy

 S.C., 0000-0002-8522-6695; G.C., 0000-0002-0628-8055

* Correspondence: giovanni.chiodini@ingv.it

Abstract: Tectonically active regions are often characterized by large amounts of carbon dioxide degassing, and estimation of the total CO₂ discharged to the atmosphere from tectonic structures, hydrothermal systems and inactive volcanic areas is crucial for the definition of present-day global Earth degassing. The carbon balance of regional aquifers is a powerful tool to quantify the diffuse degassing of deep inorganic carbon sources because the method integrates the CO₂ flux over large areas. Its application to peninsular Italy shows that the region is characterized by specific CO₂ fluxes higher than the baseline determined for the geothermal regions of the world, and that the amount of endogenous CO₂ discharged through diffuse regional degassing (*c.* 2.1×10^{11} mol a⁻¹) is the major component of the geological CO₂ budget of Italy, definitely prevailing over the CO₂ discharged by Italian active volcanoes and volcanoes with hydrothermal activity. Furthermore, the positive correlation between geothermal heat and deep CO₂ dissolved in the groundwater of central Italy suggests that (1) the geothermal heat is transported into the aquifers by the same hot CO₂-rich fluids causing the Italian CO₂ anomaly and (2) the advective heat flow is the dominant form of heat transfer of the region.

Supplementary material: The location, flow rate, extent of the hydrogeological basin, chemical and isotopic analyses of the 160 springs considered in this study, and the results of the carbon mass balance are reported in a table available at <https://doi.org/10.6084/m9.figshare.c.4237025>

Received 29 December 2017; revised 24 August 2018; accepted 14 September 2018

On geological timescales, the level of atmospheric CO₂ is controlled by the balance between CO₂ consumed by chemical weathering and CO₂ degassed by metamorphism and magmatism (Walker *et al.* 1981; Berner *et al.* 1983; Berner 1993, 2004; Kerrick & Caldeira 1993). The BLAG (Berner–LASaga–Garrels; Berner *et al.* 1983) and subsequent models for the long-term global carbon cycle (e.g. Berner 2006) derive the CO₂ degassing rate over geological times assuming that present-day CO₂ degassing equals the flux of CO₂ consumed by chemical weathering. However, the global estimates of present-day CO₂ degassing flux based on this assumption are inconsistent with those based on volcanic degassing data (Burton *et al.* 2013, and references therein), suggesting that the fluxes of CO₂ consumed by chemical weathering and those released by metamorphic–magmatic degassing should be computed separately (Fresia & Frezzotti 2015).

The number of CO₂ flux measurement studies at volcanoes is continuously increasing but the CO₂ emissions from the majority of volcanic sources are still unknown. Extrapolating the available data to all the active volcanoes, Burton *et al.* (2013) estimated a global volcanic subaerial CO₂ flux of about 12×10^{12} mol a⁻¹ and a total flux, including mid-ocean ridge degassing, of 14×10^{12} mol a⁻¹. These values are higher than previous estimates (e.g. Marty & Tolstikhin 1998; Mörner & Etiope 2002) but are still affected by large uncertainties mostly related to the estimation of diffuse degassing from inactive volcanoes and hydrothermal structures.

The impact of metamorphic degassing on the global carbon cycle is even more uncertain (Gaillardet & Galy 2008). All the estimations derive from theoretical models and studies on the Himalayan orogen (Kerrick & Caldeira 1998; Mörner & Etiope 2002; Gorman & Kerrick 2006; Rapa *et al.* 2017) but there are only few estimations of

present-day metamorphic CO₂ degassing based on direct measurements (e.g. Evans *et al.* 2008; Girault *et al.* 2016).

The so-called non-volcanic diffuse CO₂ degassing (i.e. not directly connected to active volcanoes) represents an important aspect of the global carbon cycle and its quantification is crucial to give a realistic estimate of the degassing process at a global scale (Kerrick *et al.* 1995; Chiodini *et al.* 1999, 2000, 2004b; Kerrick 2001; Lee *et al.* 2016; Hunt *et al.* 2017).

Tectonically active regions, including orogenic belts, continental rifts and, more in general, hydrothermal or inactive volcanic areas, are often characterized by widespread regional carbon dioxide degassing. In these areas carbon dioxide, derived from mantle degassing and/or metamorphism, is continuously released to the atmosphere through various processes, including emissions from focused gas vents, diffuse soil degassing, and degassing from lakes and hot and cold springs. The coincidence of carbon dioxide discharges and major zones of seismicity was first recognized by the pioneering studies of Barnes *et al.* (1978) and Irwin & Barnes (1980), and successive studies (Kerrick & Caldeira 1998) clearly showed that large orogenic belts, in addition to their role as an atmospheric CO₂ sink through silicate weathering (Gaillardet *et al.* 1999), also aid in the production of CO₂-rich fluids, mainly related to regional metamorphism. More recently, a very large amount of mantle CO₂ is hypothesized to be released by soil diffuse degassing in the East African Rift (Lee *et al.* 2016; Hunt *et al.* 2017).

A variety of techniques have been used to estimate present-day CO₂ regional degassing. In the geothermal areas of the Taupo Volcanic Zone, New Zealand, and the Salton Trough region, California, USA, the convective hydrothermal CO₂ emission was computed using data on convective heat flow, temperature and CO₂

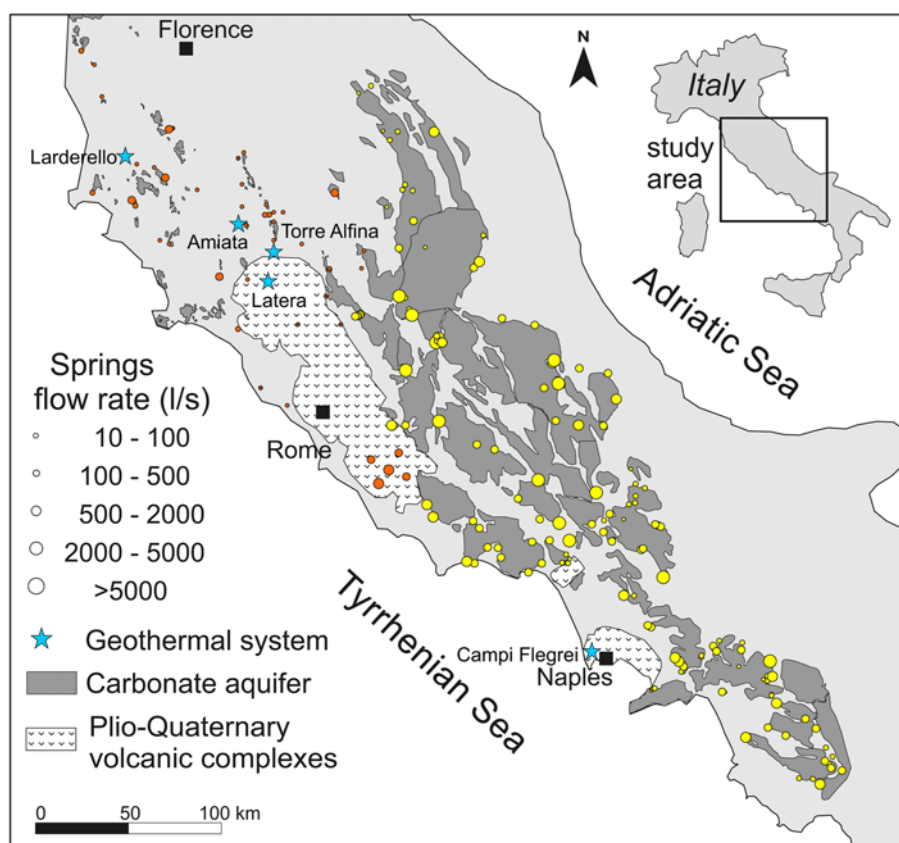


Fig. 1. Location of study area and springs from Apennine carbonate aquifers. Yellow dots refer to the Apennine springs reported in the supplementary material. Orange dots refer to springs from smaller carbonate aquifers of Umbria and Tuscany, and to Mt. Albani volcanic aquifer (from Chiodini *et al.* 2004b).

concentration of reservoir fluids (Kerrick *et al.* 1995; Seward & Kerrick 1996). The results showed that the two areas were characterized by a similar specific CO₂ flux (*c.* 10⁶ mol a⁻¹ km⁻²), and according to Kerrick *et al.* (1995) this value could be used as a baseline to compute convective hydrothermal CO₂ emission from other areas of high heat flow. However, using a similar approach, Frondini *et al.* (2008) computed a specific CO₂ flux about five times higher (4.8 × 10⁶ mol a⁻¹ km⁻²) for Tuscany and Northern Latium (Italy).

In the areas where a flux of deep CO₂ directly affects regional aquifers, most of the deeply generated gas can be dissolved in groundwater because the relatively high solubility of CO₂ in water (Rose & Davisson 1996; Sorey *et al.* 1998; Chiodini *et al.* 1999; Caliro *et al.* 2005). Hence, studying the concentration of total dissolved inorganic carbon (TDIC) in groundwater is a suitable way to infer the regional flux of endogenous CO₂.

The Earth degassing process was extensively studied in Italy and numerous techniques currently used for the estimation of non-volcanic CO₂ degassing at regional scale were originally developed for the study of the Italian territory.

At Colli Albani, central Italy (Chiodini & Frondini 2001), the CO₂ emission was computed by summing the contributions of CO₂ transported by groundwater and the CO₂ released by two large zones of diffuse soil degassing. The flux of the deeply derived CO₂ dissolved by groundwater was derived by the carbon balance of the volcanic aquifer, whereas that discharged from the areas of diffuse soil degassing was measured using the accumulation chamber method (Chiodini *et al.* 1998). The resulting area-averaged deep CO₂ production rate is 2.8 × 10⁶ mol a⁻¹ km⁻², of the same order of magnitude as the CO₂ fluxes computed by Frondini *et al.* (2004) for Tuscany and Northern Latium. Similar values were also estimated by Gambardella *et al.* (2004) for the volcanic aquifers of central-southern Italy. Chiodini *et al.* (2000, 2004b), coupled the mass and isotopic balance of TDIC with hydrogeological data from the main springs of the Italian Apennines and integrated the groundwater data

with data on vent and diffuse soil degassing, and derived a regional map of CO₂ Earth degassing that showed that two large degassing structures affect the Tyrrhenian side of the Italian peninsula and that *c.* 40% of the inorganic carbon in the groundwater derives from magmatic-mantle sources.

In this paper we discuss some of the main methods used to measure non-volcanic degassing over large areas and their application to the significant case of the Italian Apennines. In the following sections, after a brief description of the geological, hydrogeological and geophysical features of the Apennines, we will discuss (1) the methods used to measure the regional flux of deep CO₂ associated with groundwater circulation, (2) the relationships between regional flux of CO₂ and areas of focused and diffuse gas emission from soil, as well as the conditions for the development of such zones of discharge, and (3) the relationships between regional CO₂ degassing and advective heat flow.

Geological, hydrogeological and geophysical setting

The Apennines are a series of mountain ridges that run the entire length of the Italian Peninsula, extending from Liguria (northern Italy) to Sicily. They form the physical backbone of peninsular Italy and are divided into three sectors: northern, central and southern Apennines. The study area (Fig. 1), delimited to the west by the Tyrrhenian coastline, includes the central Apennines and part of the northern and southern Apennines.

The stratigraphical successions of the Apennines are essentially composed by shallow-water carbonate platform formations and pelagic formations (limestones and marly limestones), followed by foredeep deposits (arenaceous turbidites, marls and calcarenites). The present structural setting of the Apennines is the result of the superimposition, since the Early Miocene, of two concurrent tectonic processes, compression in the foreland and extension in the hinterland. The two processes are co-axial and both are characterized by an eastward migration over time. As the result of this

tectonic evolution, the Apennines show two different crustal domains: a western Tyrrhenian domain, where extensional deformation destroyed the pre-existing compressional belt, and an eastern Adriatic domain, where the compressional structures are still preserved (Barchi 2010; Cosentino *et al.* 2010).

Crustal thinning related to extension in the Tyrrhenian area was followed by intense magmatic activity along the western margin of the Italian peninsula. Igneous rocks, ranging in age from Late Miocene to Recent, are widespread through the Tyrrhenian extensional zone (Barberi *et al.* 1971; Civetta *et al.* 1978; Peccerillo 1999; Peccerillo & Frezzotti 2015).

The western Tyrrhenian domain is characterized by a thin crust (0–25 km), high heat flow, locally more than 200 mW m⁻² (Della Vedova *et al.* 1984), positive magnetic anomalies (Arisi Rota & Fichera 1985), shallow earthquakes and positive gravity anomaly. The most important Italian geothermal fields (e.g. Larderello, Amiata, Latera, Torre Alfina and Campi Flegrei) are located in this region (Fig. 1).

The eastern Adriatic domain is characterized by lower heat flow values, negative gravity anomalies and an average crustal thickness of about 35 km. This area is also characterized by high seismicity, which has caused several strong earthquakes in recent times (Amato *et al.* 1998; Chiarabba *et al.* 2009; Chiaraluce *et al.* 2017).

The hydrogeological settings of the western Tyrrhenian and eastern Adriatic domains reflect the differences described above: the western region is characterized by small shallow aquifers hosted by Quaternary volcanic rocks and small isolated carbonate structures deriving from the disruption of the pre-existing compressional structures; in contrast, the eastern region is characterized by large regional aquifers hosted by Mesozoic permeable limestones (e.g. Boni *et al.* 1986).

CO₂ degassing in peninsular Italy

Several regional-scale studies showed that the western Tyrrhenian domain is affected by intense CO₂ degassing, which results in numerous cold, CO₂-rich gas emissions at the surface (e.g. Chiodini *et al.* 2000, 2004b, 2011; Rogie *et al.* 2000; Minissale 2004). Different techniques were used to measure the gas flux depending on the specific features of each gas emission. For a detailed description of these methods, the reader is referred to the specific literature (Chiodini *et al.* 1998, 2010; Rogie *et al.* 2000; Cardellini *et al.* 2003; Costa *et al.* 2008). The measured gas flow rates in some cases are very high, as, for example, at Mefite d'Ansanto, the largest cold CO₂ emission ever measured on Earth, which releases amounts of CO₂ (c. 1.7 × 10¹⁰ mol a⁻¹) approaching those released from the most active volcanoes (Chiodini *et al.* 2010).

The idea of measuring CO₂ flux at regional scale derived from the observation that the main Apennine springs emit large amounts of dissolved CO₂. In principle, the spring discharge can be used to estimate the specific CO₂ fluxes over large areas; that is, the areas of the hydrogeological basins. However, before computing the CO₂ fluxes from TDIC it is essential to define the origin of the dissolved gas in water because in addition to a possible deeply derived component, atmospheric sources, biogenic activity and water–rock interactions contribute to TDIC. This aspect is solved by applying the mass-balance approach described below.

Materials and methods

Data

The dataset used in this study (supplementary material) refers to 160 Apennine springs (Fig. 1) that were sampled in different surveys (Civita 1977; Celico *et al.* 1980; Chiodini *et al.* 2000, 2004b, 2013; Frondini *et al.* 2012). Water temperature, pH and total alkalinity were

determined directly in the field. The chemical (Ca, Mg, Na, K, Cl, SO₄, NO₃) and stable isotope (H₂O and carbon) composition was determined according to the analytical methods reported in the original studies. The TDIC was computed with the code PHREEQC (Parkhurst & Appelo 1999), using the field determinations of *T*, pH and alkalinity, and the major ion concentrations as input data. For each sample two additional variables (C_{ext} and δ¹³C_{ext}; supplementary material) were computed according to the method explained in the next section.

The strategy of the survey was to sample the high-discharge springs to obtain a dataset highly representative of the Apennines groundwater. The flow rates of the springs and the areal coverage for the corresponding hydrogeological basins (supplementary material) were taken from the literature (Celico *et al.* 1979; Celico & Corniello 1980; Celico 1983; Boni *et al.* 1986).

Carbon mass balance of the aquifers

To compute the flux of endogenous CO₂ transported by groundwater it is necessary to discriminate the different sources of dissolved carbon dioxide. A theoretical treatment of the evolution of the carbon isotopes in natural waters has been given by Wigley *et al.* (1978). The effects of an arbitrary number of sources (such as dissolution of carbonate minerals, input of deeply derived CO₂, oxidation of organic material) and sinks (such as mineral precipitation and CO₂ degassing), and equilibrium fractionation between solid, gas and aqueous phases are considered. The results are expressed as equations relating changes in isotopic composition to changes in carbonate chemistry.

The evolution of the TDIC and ¹³C/¹²C ratio of natural water systems is described by the following equations:

$$d(\text{TDIC}) = \sum_{i=1}^N dI_i - \sum_{i=1}^M dO_i \quad (1)$$

$$d(R_{\text{TDIC}}) = \sum_{i=1}^N R_i^* dI_i - \sum_{i=1}^M R \alpha_{i-s} dO_i \quad (2)$$

where *I_i* and *O_i* are the molalities of the *i*th input and the *i*th output of carbon in the solution, *R* is the ¹³C/¹²C isotopic ratio of the solution as a whole, *R** is the ¹³C/¹²C isotopic ratio of the *i*th input species, α_{*i-s*} is the fractionation factor between the *i*th output and the solution, and *N* and *M* are the numbers of incoming and outgoing carbon species. For a finite-difference solution, equation (1) becomes

$$\Delta(\text{TDIC}) = \sum_{i=1}^N \Delta I_i - \sum_{i=1}^M \Delta O_i \quad (3)$$

and equation (2), considering the isotopic values in terms of delta units, becomes

$$\begin{aligned} & \delta^{13}\text{C}_{\text{TDIC}} + \Delta(\delta^{13}\text{C}_{\text{TDIC}}) \\ &= \frac{(\delta^{13}\text{C}_{\text{TDIC}} + 1000)(\text{TDIC} - \sum_{i=1}^M \alpha_{i-s} \Delta O_i)}{\text{TDIC} + \Delta(\text{TDIC})} \\ &+ \frac{\sum_{i=1}^N (\delta^{13}\text{C}_i^* + 1000) \Delta I_i}{\text{TDIC} + \Delta(\text{TDIC})} - 1000 \end{aligned} \quad (4)$$

In equations (2) and (4) it is assumed that isotopic equilibrium exists between all dissolved carbon species in solution and that all outputs are in isotopic equilibrium with the parent solution. Furthermore, it is assumed that no fractionation occurs during the input of any source to the solution, and fractionation occurs only during the output of carbon from the parent solution.

In the case of the regional Apennines aquifers, equations (3) and (4) were rearranged assuming that no carbon sinks are present in the aquifer, an assumption that was demonstrated to be realistic for most of the studied springs (Chiodini *et al.* 2000, 2011). In the case of

carbonate aquifers, the no-sink assumption means that carbonate precipitation and CO₂ degassing do not significantly occur before the emergence of groundwater at springs. In this case the amount of carbon dissolved by groundwater is given by the sum of the carbon deriving from carbonate dissolution and the carbon deriving from sources external to the aquifer. It is possible to eliminate the contribution of carbonate dissolution (C_{carb}) to TDIC by computing two new variables, C_{ext} and $\delta^{13}\text{C}_{\text{ext}}$:

$$C_{\text{ext}} = \text{TDIC} - C_{\text{carb}} \quad (5)$$

$$\delta^{13}\text{C}_{\text{ext}} = \frac{\delta^{13}\text{C}_{\text{TDIC}} \times \text{TDIC} - \delta^{13}\text{C}_{\text{carb}} \times C_{\text{carb}}}{C_{\text{ext}}} \quad (6)$$

where C_{ext} is given by the sum of the carbon deriving from a deep source (C_{deep}) and the carbon content of infiltrating waters (C_{inf} ; i.e. the atmospheric CO₂ plus that from biogenic sources active in the soils during the infiltration):

$$C_{\text{ext}} = C_{\text{inf}} + C_{\text{deep}} \quad (7)$$

from which derives

$$\delta^{13}\text{C}_{\text{ext}} = \frac{\delta^{13}\text{C}_{\text{inf}} \times C_{\text{inf}} + \delta^{13}\text{C}_{\text{deep}} \times C_{\text{deep}}}{C_{\text{ext}}} \quad (8)$$

where $\delta^{13}\text{C}_{\text{inf}}$ and $\delta^{13}\text{C}_{\text{deep}}$ correspond to the isotopic composition of C_{inf} and C_{deep} respectively.

In the above set of equations, only the TDIC and $\delta^{13}\text{C}_{\text{TDIC}}$ are analytically determined whereas the other variables are derived from general considerations and from the geochemical interpretation of the data.

For example, in the carbonate aquifers of the Apennines, C_{carb} is given by

$$C_{\text{carb}} = m\text{Ca} + m\text{Mg}_m\text{SO}_4 \quad (9)$$

Equation (9) states that the moles of C_{carb} are equivalent to the moles of Ca and Mg entering the solution from carbonate mineral dissolution, and the negative term $-m\text{SO}_4$ corrects for the moles of Ca in solution that were derived from gypsum or anhydrite dissolution. In the case of aquifers composed of silicate crystalline rocks or volcanic rocks, the contribution of carbonate dissolution to TDIC may be assumed negligible and C_{ext} is equal to TDIC.

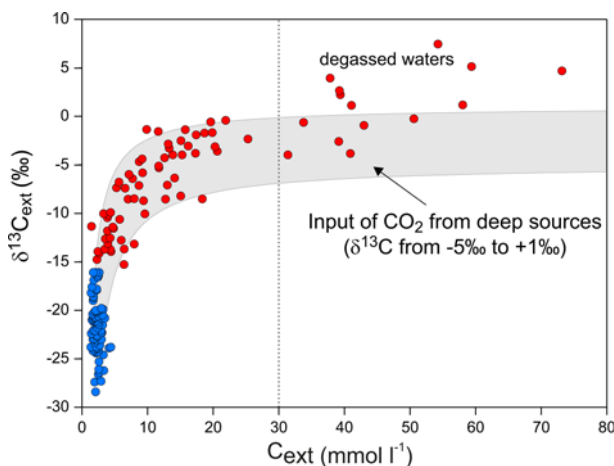


Fig. 2. C_{ext} v. $\delta^{13}\text{C}_{\text{ext}}$ diagram. Blue circles refer to groundwater with a C_{ext} and $\delta^{13}\text{C}_{\text{ext}}$ compatible with dissolution of biological CO₂ only, whereas red circles refer to groundwater with a high C_{ext} and $\delta^{13}\text{C}_{\text{ext}}$ compatible with some input of deeply derived CO₂. The theoretical field resulting from the addition of C_{deep} with $\delta^{13}\text{C}_{\text{deep}}$ ranging from -5 to $+1$ ‰ to infiltrating water with $C_{\text{inf}} = 2.31 \pm 0.61 \text{ mmol l}^{-1}$ and $\delta^{13}\text{C}_{\text{inf}} = -21.6 \pm 2.9$ ‰ is indicated in grey. The dashed vertical line represents the C_{ext} upper limit for the applicability of the no-sink assumption.

$\delta^{13}\text{C}_{\text{carb}}$ is the carbon isotopic composition of the carbonate rocks and preferably should be determined based on known values for the carbonate rocks that host the aquifers (e.g. in the Apennine aquifers it was assumed to be $+2.21$ ‰, based on hundreds of isotopic analyses of carbonate rocks; Chiodini *et al.* 2004b).

The values of C_{carb} and $\delta^{13}\text{C}_{\text{carb}}$ allow one to compute C_{ext} and $\delta^{13}\text{C}_{\text{ext}}$ (from equations (5) and (6)). The other unknown variables (C_{inf} , C_{deep} , $\delta^{13}\text{C}_{\text{inf}}$ and $\delta^{13}\text{C}_{\text{deep}}$) are computed from equations (7) and (8), by making suitable assumptions constrained by the geochemical interpretation of the data.

Once all the terms of the carbon budget are determined (C_i), the total output of CO₂ ($Q_{\text{CO}_2,i}$) and the corresponding CO₂ flux ($F_{\text{CO}_2,i}$) can be computed for any carbon source using the following equations:

$$Q_{\text{CO}_2,i} = C_i \times q \quad (10)$$

$$F_{\text{CO}_2,i} = Q_{\text{CO}_2,i}/A \quad (11)$$

where q is the spring flow rate and A is the surface area of the hydrogeological basin of the spring.

The case of the Apennine aquifers is described below.

Results and discussion

Carbon mass balance of Apennines aquifers

The computation of C_{deep} is based on the analysis of the C_{ext} v. $\delta^{13}\text{C}_{\text{ext}}$ diagram (Fig. 2) where data from the Apennines springs are distributed along mixing lines consistent with expected theoretical behaviour and calculated using equations (7) and (8). A cluster of samples (blue circles in Fig. 2; described as blue samples below) is characterized by low C_{ext} values ($<3-4 \text{ mmol l}^{-1}$) and very negative $\delta^{13}\text{C}_{\text{ext}}$ (from -16 to -25 ‰). These are the springs where C_{deep} is absent (or negligible) and where C_{ext} practically coincides with C_{inf} . Most of the other samples (red circles in Fig. 2) show an enrichment in C_{ext} and higher $\delta^{13}\text{C}_{\text{ext}}$ values, indicative of the addition of isotopically heavier carbon, typical of endogenous sources (i.e. the deeply derived C_{deep}). The C_{inf} values of the blue samples range in a narrow interval and the mean value ($2.31 \pm 0.61 \text{ mmol l}^{-1}$) can be assumed as representative of the recharge waters of the Apennines. Using this value in equation (7) we can compute C_{deep} for each spring affected by the input of deep CO₂ (red circles in Fig. 2). In this computation, for the few samples where C_{ext} is lower than the mean C_{inf} value, we assumed $C_{\text{deep}} = 0$.

Alternatively, C_{deep} can be computed assuming (or evaluating) the isotopic compositions of the pure components. This method, described by Chiodini *et al.* (2011), is generally applicable in areas where one can assume the deep carbon source has a unique isotopic signature.

To characterize the isotopic signature of the deep carbon sources in the Apennines, we have to consider that the no-sink assumption, which is necessary for application of this method, is realistic only for samples characterized by TDIC $<40 \text{ mmol l}^{-1}$ (which roughly corresponds to a C_{ext} of $c. 30 \text{ mmol l}^{-1}$; dashed line in Fig. 2). This threshold was defined by Chiodini *et al.* (2011) modelling the effects of CO₂ input on the dissolved carbon species of water at equilibrium with calcite. Above this threshold samples could be affected by CO₂ degassing and calcite precipitation, which can cause significant isotopic fractionation and a decrease of C_{ext} (i.e. it would not be representative of mixing between C_{inf} and C_{deep}). Figure 2 shows that samples with C_{ext} lower than the no-sink threshold plot in the theoretical mixing field computed by adding to the infiltrating water ($C_{\text{inf}} = 2.31 \pm 0.61 \text{ mmol l}^{-1}$; $\delta^{13}\text{C}_{\text{inf}} = -21.6 \pm 2.9$ ‰) variable amounts of C_{deep} with $\delta^{13}\text{C}_{\text{deep}}$ ranging

from -5 to $+1\%$, the typical range of deeply derived CO_2 emitted in Italy by volcanoes, geothermal systems and cold CO_2 emissions (Chiodini *et al.* 2004b).

The estimated concentrations of the different carbon sources multiplied by the flow rate of the springs (equation (10)) give the total output of CO_2 associated with the Apennines groundwater as follows: $Q_{\text{CO}_2, \text{carb}} = 2.2 \times 10^{10} \text{ mol a}^{-1}$, $Q_{\text{CO}_2, \text{inf}} = 1.6 \times 10^{10} \text{ mol a}^{-1}$ and $Q_{\text{CO}_2, \text{deep}} = 2.9 \times 10^{10} \text{ mol a}^{-1}$. It is noteworthy that the results show that the deep source of CO_2 is the main source supplying inorganic carbon to the Apennine groundwaters.

Regional map of CO_2 Earth degassing

To derive the map of the regional CO_2 flux, following the approach of Chiodini *et al.* (2004b), the dataset of the Apennine springs was integrated with literature data for springs from smaller carbonate aquifers in the western part of Italy (with flow rates $>10 \text{ l s}^{-1}$). Furthermore, we also considered in the computation the average CO_2 flux affecting the volcanic aquifer of Mt. Albani, as previously estimated by Chiodini & Frondini (2001). Starting from the C_{ext} values derived from equation (5), the CO_2 flux of each spring (in $\text{mol a}^{-1} \text{ km}^2$) was computed by multiplying its C_{ext} by the corresponding flow rate and dividing the result by the surface area of its hydrogeological basin (equations (10) and (11)). The CO_2 fluxes computed for each spring were subsequently determined using a geostatistical approach based on the sequential Gaussian simulation procedure (sGs; Deutsch & Journel 1998), which frequently is applied to derive maps of soil CO_2 diffuse degassing from field measurements (e.g. Cardellini *et al.* 2003). In this study, each spring was considered as a single CO_2 flux measurement point for the application of the sGs algorithm and the derivation of the regional map. We computed 200 maps of CO_2 flux by sGs according to the geostatistical parameters of the dataset (a spherical variogram model with nugget = 0.35, sill = 1 and range = 50 km), weighting each datum point for the spring flow rate. The average values computed from the 200 simulations at each location are shown in the map of Figure 3. The map highlights the presence of two large regional anomalies of CO_2 flux on the western side of the Italian peninsula: the Tuscan Roman Degassing Structure and the Campanian Degassing Structure (TRDS and CDS in Fig. 3;

Chiodini *et al.* 2004b). On the map the areas degassing deeply derived CO_2 are shown by colours from light green to red, corresponding to C_{ext} flux values higher than $3 \times 10^6 \text{ mol a}^{-1} \text{ km}^{-2}$. This threshold was computed considering a reasonable maximum value for C_{inf} of biological origin (c. 0.004 mol l^{-1} , Chiodini *et al.* 2004b) and using equations (10) and (11) to convert concentration into flux.

The northern degassing structure (TRDS) partially overlaps the Tuscany, Roman magmatic provinces whereas the southern structure (CDS) is related to areas of Campanian volcanism. The two volcanic provinces are characterized by Quaternary potassic and ultrapotassic magmas rich in fluids with high $\text{CO}_2/\text{H}_2\text{O}$ ratios (Foley 1992). Magma geochemistry is consistent with the melting of a mantle source metasomatized by the addition of subducted crustal material (e.g. Peccerillo 1999; Frezzotti *et al.* 2009). In agreement with Chiodini *et al.* (2004b, 2011) we suggest that the TRDS and CDS mostly reflect degassing of this metasomatized mantle.

It should be noted that the real existence of the TRDS and CDS is confirmed by the presence of numerous (c. 140) widespread CO_2 -rich gas emissions consisting of cold gas vents, areas of soil diffuse degassing and bubbling waters (Fig. 3; www.magadb.net). In particular, the free gas emissions occur in the western sectors of the TRDS and CDS, which are characterized by outcrops of relatively low-permeability formations, whereas in the eastern sectors, where permeable carbonate formations prevail, the deeply derived gas is almost completely dissolved by groundwater circulating in the Apennine aquifers.

The total amount of deeply derived carbon released from the TRDS and CDS was estimated by integrating the simulated CO_2 flux values (i.e. C_{ext}) over the area and subtracting the contribution from the atmospheric and organic sources (i.e. C_{inf}). This computation assumes a mean recharge water infiltration of $20 \text{ l s}^{-1} \text{ km}^{-2}$, and gives a deep carbon flux of $1.4 \times 10^{11} \text{ mol a}^{-1}$ for the TRDS and $0.7 \times 10^{11} \text{ mol a}^{-1}$ for the CDS, corresponding to deeply derived specific CO_2 fluxes of c. $3.7 \times 10^6 \text{ mol a}^{-1} \text{ km}^{-2}$ and c. $4.7 \times 10^6 \text{ mol a}^{-1} \text{ km}^{-2}$, respectively. The total amount of deeply derived CO_2 discharged by this sector of Italy (c. $2.1 \times 10^{11} \text{ mol a}^{-1}$) corresponds to about 2–15% of the estimated present-day global CO_2 fluxes from active volcanoes (Burton *et al.* 2013),

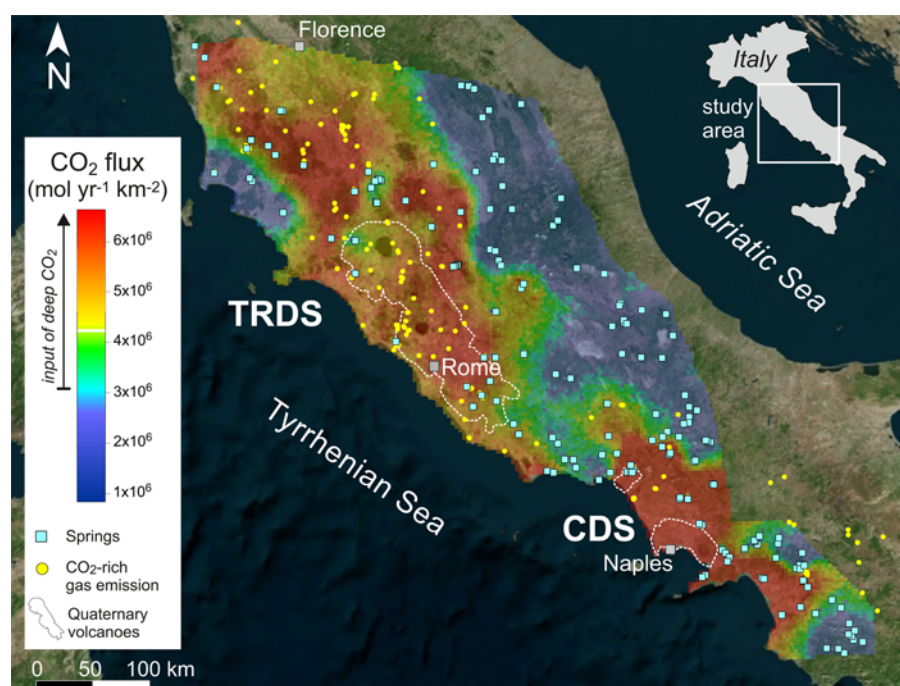


Fig. 3. Regional map of CO_2 degassing. The map reports the CO_2 flux estimated through a geostatistical approach starting from the C_{ext} values of each spring, the locations of which are indicated by open squares. Dashed lines highlight the location of Quaternary volcanic areas. The locations of CO_2 -rich gas emissions are shown as yellow circles (from www.magadb.net).

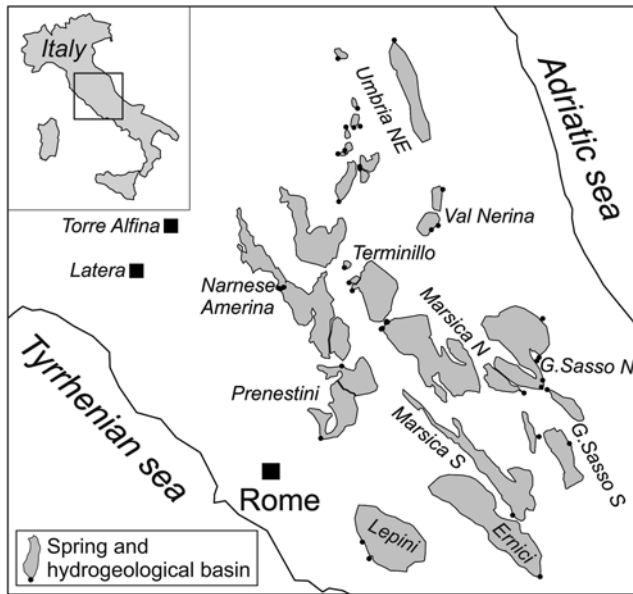


Fig. 4. Location of the central Italy Apennine aquifers showing locations where estimates of the advective heat flux have been calculated (Chiodini *et al.* 2013).

highlighting the global relevance of the regional CO₂ Earth degassing process in the region. Finally, the computed specific CO₂ fluxes are 4–5 times higher than the value of $c. 10^6 \text{ mol a}^{-1} \text{ km}^{-2}$ suggested as the reference value for the convective hydrothermal CO₂ emission calculated for high heat flow areas (Kerrick *et al.* 1995).

Advective heat transport and CO₂ fluxes

On the heat flux map of Italy the Apennine portions of the TRDS and CDS correspond to zones of apparently very low heat flux (Cataldi *et al.* 1995). However, this map refers only to the conductive heat flux because the map is based on temperature gradients measured in wells. In regions characterized by permeable rocks that host large aquifers, such as the Apennines, groundwater circulation invalidates use of a purely conductive model to estimate heat flux. Instead, because of the abundant groundwater circulation, advective heat flow can be the dominant form of heat transfer, and the temperature of spring water can be used to estimate the values of geothermal heat flux more realistically with

Table 1. Geothermal heat (Q_H) and total CO₂ release ($Q_{\text{CO}_2, \text{deep}}$) from the aquifers of central Italy, from the Matese aquifer and from the geothermal systems of Latera and Torre Alfina (Fig. 4)

Name	Q_H (MW)	$Q_{\text{CO}_2, \text{deep}}$ (mol a ⁻¹)
Umbria NE	9.3	0
Val Nerina	4.1	0
Terminillo	13.2	0
Narnese–Amerina	259.4	6.7×10^9
Marsica N	202.2	3.6×10^9
G Sasso N	139.9	1.3×10^9
G Sasso S	12.2	0
Prenestini	184.3	5.0×10^9
Ernici	195.5	2.5×10^9
Marsica S	91.9	1.1×10^9
Lepini	163.7	2.7×10^9
Matese	47.3	3.3×10^9
Latera	117.0	2.9×10^9
Torre Alfina	31.0	0.7×10^9

respect to the estimations made using the thermal gradients measured in deep wells. A method based on the energy balance of groundwater was applied to the US Cascade Range, allowing the identification of a deep thermal source active in the area (e.g. Ingebritsen *et al.* 1989; Manga 1998; Ingebritsen & Mariner 2010). More recently, Chiodini *et al.* (2013) used the same method to estimate the advective geothermal heat flux (together with the CO₂ flux) for 11 aquifers of the central Apennines belonging to the TRDS (Fig. 4).

Briefly, the geothermal heat flux (F_H) is computed starting from ΔT , the temperature difference between the recharge water and the water discharged from the springs. In particular, the method considers the effect on water temperature for both geothermal heating and dissipation of gravitational potential energy (Manga & Kirchner 2004). Assuming that the effect of the conductive heat transfer from the aquifer to the surface is negligible, a reasonable assumption for aquifers with a water table at depths higher than 100 m, the temperature difference between the discharge (T_s) and the infiltration water (T_r), ΔT (in K), is given by

$$\Delta T = T_s - T_r = (F_H)/(\rho_w \times C_w) \times A/q + \Delta z \times (g/C_w) \quad (12)$$

where F_H is the geothermal heat flux (in W m^{-2}), ρ_w (kg m^{-3}) and C_w ($\text{J kg}^{-1} \text{K}^{-1}$) are the density and the heat capacity of water respectively, A is the areal extent of the hydrogeological basin covered by each spring (m^2), q is the spring flow rate ($\text{m}^3 \text{s}^{-1}$), Δz (m) is the difference in elevation between the water recharge area (Z_r) and the spring (Z_s), and g is the gravitational acceleration (m s^{-2}). In equation (12), the first term relates to the geothermal heating and the second relates to the dissipation of gravitational potential energy.

The total amount of geothermal heat released by an aquifer is given by

$$Q_H = F_H \times A \quad (13)$$

In Table 1 we show the total geothermal heat (Q_H) and the CO₂ ($Q_{\text{CO}_2, \text{deep}}$) outputs computed for 11 aquifers of the TRDS by Chiodini *et al.* (2013) and for one aquifer of the CDS (Matese aquifer; Di Luccio *et al.* 2018). For further details on the method and on the computation of the variables in equations (12) and (13) we refer the reader to the original studies.

The Q_H and $Q_{\text{CO}_2, \text{deep}}$ values estimated for the 12 aquifers show a positive correlation (Fig. 5), suggesting that the gas and the heat are advectively transported into the aquifers by hot CO₂-rich fluids. It is noteworthy that the original fluids have a Q_H/Q_{CO_2} ratio similar to that of the hot liquids circulating in the nearby geothermal systems

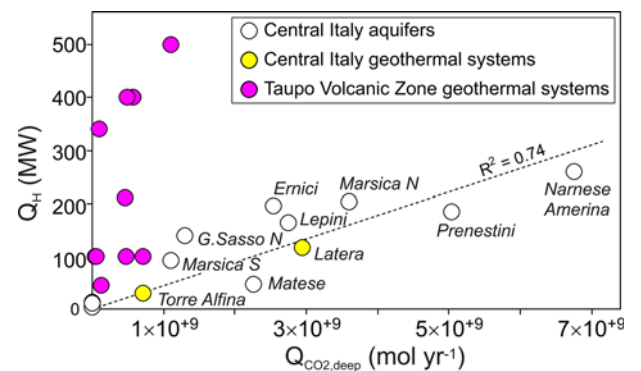


Fig. 5. The total geothermal heat (Q_H) plotted v. total CO₂ of deep origin ($Q_{\text{CO}_2, \text{deep}}$) that enters the 11 aquifers of the central Apennines (Fig. 4) and the Matese aquifer. All the aquifers are labelled except Umbria NE, G. Sasso S and Terminillo, that plot close to the origin. The Q_H and Q_{CO_2} associated with geothermal systems in central Italy and in the Taupo Volcanic Zone (Kerrick *et al.* 1995) are reported for comparison.

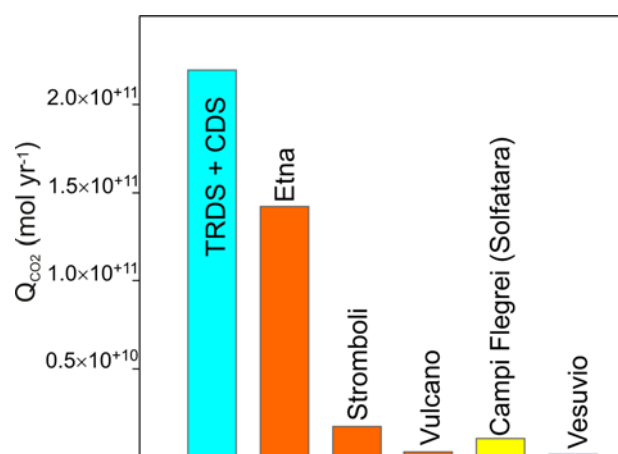


Fig. 6. Output of deeply derived CO₂ in Italy from volcanoes with hydrothermal systems (yellow), volcanoes emitting SO₂ (red), and from regional diffuse degassing structures in central Italy (blue).

of Latium (Latera and Torre Alfina; Figs 4 and 5). The total CO₂ output from the two geothermal systems (Table 1) was estimated through hundreds of CO₂ flux measurements performed with the accumulation chambers technique (Chiodini *et al.* 2007; Lucidi 2010). Considering the temperature and the CO₂ contents of the geothermal liquids at Torre Alfina (120°C, 0.37 mol kg⁻¹; Gambardella *et al.* 2004) and Latera (212°C, 0.72 mol kg⁻¹; Chiodini *et al.* 2007) we estimated Q_H of the two systems, computing the total amount of liquid necessary to supply the measured Q_{CO_2} and multiplying it by the specific enthalpy of the liquid at the measured temperature.

For comparison, in Figure 5 are also reported the data from the geothermal Taupo Volcanic Zone (TVZ) that were used by Kerrick *et al.* (1995) to derive the specific CO₂ flux value of $c. 10^6 \text{ mol a}^{-1} \text{ km}^{-2}$ assumed by those researchers as the baseline for the convective hot zones of the Earth. Figure 5 explains well why in central Italy the specific CO₂ fluxes are 4–5 times higher than those derived from TVZ data: the central Italy original fluids have a Q_H/Q_{CO_2} ratio that is much lower than that in the TVZ.

Conclusion

A main goal of modern geoscience is to better define and quantify the geological components of the global carbon cycle. In particular, the amount of CO₂ derived from inorganic sources (mantle, crust) and released to the atmosphere is a central parameter that at the moment is known only with large uncertainties. A special study has been made recently to quantify the CO₂ emitted by the plumes of volcanoes (DCO DECADE initiative, <https://deepcarboncycle.org/about-decade>). However, no effort has been devoted to understanding and quantifying diffuse degassing, whose contribution to the total CO₂ flux to the atmosphere is practically unknown, despite some appreciable but local research.

Here we have shown that knowledge of the carbon balance of an aquifer is a powerful tool to quantify the diffuse degassing of deep inorganic carbon sources. The results of the carbon balance of aquifers can give the average CO₂ flux over large areas (typically of tens to hundreds of square kilometres in the Apennines).

The application of the method in Italy shows that the specific CO₂ fluxes (i.e. $c. 3.7 \times 10^6 \text{ mol a}^{-1}$ in the TRDS and $c. 4.7 \times 10^6 \text{ mol a}^{-1}$ in the CDS) are higher than the reference baseline specific CO₂ flux for hot, hydrothermal zones of the Earth (10^6 mol a^{-1} ; Kerrick *et al.* 1995). This could reflect a real strong CO₂ anomaly in Italy and/or a difference in the method of computation. It should be noted that the method based on the carbon

and heat balance of the aquifers (Table 1, Fig. 5) refers to a natural steady-state condition of the process of ascent of hot, CO₂-rich fluids and their consequent mixing with shallow groundwater. On the other hand, the method based on data from deep geothermal wells (i.e. Kerrick *et al.* 1995) could be affected by the perturbation of the steady-state condition caused by the extraction of the geothermal fluids. It should be noted that the two geothermal systems of central Italy (Latera and Torre Alfina), which give results comparable with those returned by the aquifers, were exploited only for short periods and are currently unexploited.

Finally, the total amount of deeply derived CO₂ ($c. 2.1 \times 10^{11} \text{ mol a}^{-1}$) released by the TRDS and CDS, the two degassing structures located in peninsular Italy (Fig. 3), is the main component (55%) of the geological CO₂ budget of Italy (Fig. 6) including the SO₂-bearing plumes of active volcanoes (Etna, Stromboli, Vulcano; Burton *et al.* 2013) and the volcanoes with hydrothermal activity where SO₂ is practically absent (Campi Flegrei and Vesuvio; Frondini *et al.* 2004; Cardellini *et al.* 2017). The inclusion in the budget of other hydrothermal systems, such as Ischia and Pantelleria, where CO₂ flux estimates are minor with respect to the total budget (and may also be affected by large uncertainties; Favara *et al.* 2001; Chiodini *et al.* 2004a; Pecoraino *et al.* 2005; Granieri *et al.* 2014), would not change this picture of the diffuse degassing as the main natural producer of inorganic geological CO₂ in Italy.

The results obtained in Italy demonstrate that total CO₂ flux estimates cannot be reliably quantified without the investigation of groundwaters, which in permeable orogens of tectonically young and active areas can dissolve most, if not all, the CO₂ rising from depth. Although it has long been recognized (Barnes *et al.* 1978; Irwin & Barnes 1980) that seismically active regions worldwide are characterized by the occurrence of CO₂ degassing, quantitative data on CO₂ fluxes are practically missing for most of these. We believe that investigation of diffuse degassing in these regions is crucial to better constrain the global carbon flux.

Funding This work was funded by the Istituto Nazionale di Geofisica e Vulcanologia.

Scientific editing by Igor Maria Villa

References

- Amato, A. *et al.* 1998. The 1997 Umbria–Marche, Italy, Earthquake Sequence: A first look at the main shocks and aftershocks. *Geophysical Research Letters*, **25**, 1861–1864.
- Arisi Rota, F. & Fichera, R. 1985. Magnetic interpretation connected to geomagnetic provinces: the Italian case history. *In*: 47th Meeting European Association of Exploration Geophysicists Proceedings, Budapest, Hungary, 4–7 June 1985. Blackwell Science.
- Barberi, F., Innocenti, F. & Ricci, C.A. 1971. Il magmatismo nell'Appennino centro-settentrionale: La Toscana Meridionale. *Rendiconti della Società Italiana di Mineralogia e Petrologia*, **27**, 169–210.
- Barchi, M. 2010. The Neogene–Quaternary evolution of the Northern Apennines: crustal structure, style of deformation and seismicity. *Journal of the Virtual Explorer*, **36**, paper 11, <https://doi.org/10.3809/jvirtex.2010.00220>
- Barnes, I., Irwin, W.P. & White, D.E. 1978. *Global distribution of carbon-dioxide discharges, and major zones of seismicity, scale 1:40,000,000*. US Geological Survey, Water Resources Investigation Report, **WRI 78-39**.
- Berner, R.A. 1993. Weathering and its effect on atmospheric CO₂ over Phanerozoic time. *Chemical Geology*, **107**, 373–374, [https://doi.org/10.1016/0009-2541\(93\)90212-2](https://doi.org/10.1016/0009-2541(93)90212-2)
- Berner, R.A. 2004. *The Phanerozoic Carbon Cycle: CO₂ and O₂*. Oxford University Press, Oxford.
- Berner, R.A. 2006. GEOCARBSULF: A combined model for Phanerozoic atmospheric O₂ and CO₂. *Geochimica et Cosmochimica Acta*, **70**, 5653–5664, <https://doi.org/10.1016/j.gca.2005.11.032>
- Berner, R.A., Lasaga, A.C. & Garrels, R.M. 1983. The carbonate–silicate geochemical cycle and its effect on atmospheric carbon dioxide over the past 100 million years. *American Journal of Science*, **283**, 641–683, <https://doi.org/10.2475/ajs.283.7.641>
- Boni, C.F., Bono, P. & Capelli, G. 1986. Schema Idrogeologico dell'Italia Centrale. *Memorie della Società Geologica Italiana*, **35**, 991–1012.

- Burton, M.R., Sawyer, G.M. & Granieri, D. 2013. Deep carbon emissions from volcanoes. In: Hazen, R.M., Jones, A.P. & Baross, J.A. (eds) *Carbon in Earth*. Mineralogical Society of America and Geochemical Society, Reviews in Mineralogy and Geochemistry, **75**, 323–354, <https://doi.org/10.2138/rmg.2013.75.11>
- Caliro, S., Chiodini, G., Avino, R., Cardellini, C. & Frondini, F. 2005. Volcanic degassing at Somma–Vesuvio (Italy) inferred by chemical and isotopic signatures of groundwater. *Applied Geochemistry*, **20**, 1060–1076, <https://doi.org/10.1016/j.apgeochem.2005.02.002>
- Cardellini, C., Chiodini, G. & Frondini, F. 2003. Application of stochastic simulation to CO₂ flux from soil: mapping and quantification of gas release. *Journal of Geophysical Research*, **108**, 2425, <https://doi.org/10.1029/2002JB002165>
- Cardellini, C., Chiodini, G. *et al.* 2017. Monitoring diffuse volcanic degassing during volcanic unrests: the case of Campi Flegrei (Italy). *Scientific Reports*, **7**, 6757, <https://doi.org/10.1038/s41598-017-06941-2>
- Cataldi, R., Mongelli, F., Squarci, P., Taffi, L., Zito, G. & Calore, C. 1995. Geothermal ranking of Italian territory. *Geothermics*, **24**, 115–129.
- Celico, P. 1983. Idrogeologia dell'Italia centro-meridionale. *Quaderni della Cassa del Mezzogiorno*, **4**. Cassa del Mezzogiorno, Roma.
- Celico, P. & Comiello, A. 1980. Idrodinamica, potenzialità e possibilità di sfruttamento delle risorse idriche sotterranee dei monti Lattari (Campania). In: Nicotera, P. (ed.) *Memorie e note dell'Istituto di Geologia Applicata dell'Università di Napoli*, **15**, 5–24.
- Celico, P., De Gennaro, M., Ghiara, M.R. & Stanzione, D. 1979. Le sorgenti termominerali della Valle del Sele (Salerno). Indagini strutturali, idrogeologiche e geochemiche. *Rendiconti della Società Italiana di Mineralogia e Petrologia*, **35**, 389–409.
- Celico, P., De Gennaro, M., Ferreri, M., Ghiara, M.R., Rosso, D., Stanzione, D. & Zenone, F. 1980. Il margine orientale della Piana Campana: Indagini idrogeologiche e geochemiche. *Periodico di Mineralogia*, **49**, 241–270.
- Chiarabba, C. *et al.* 2009. The 2009 L'Aquila (central Italy) M_w 6.3 earthquake: Main shock and aftershocks. *Geophysical Research Letters*, **36**, L18308, <https://doi.org/10.1029/2009GL0396>
- Chiaraluze, L., Di Stefano, R. *et al.* 2017. The 2016 Central Italy Seismic Sequence: A First Look at the Mainshocks, Aftershocks, and Source Models. *Seismological Research Letters*, **88**, 757–771, <https://doi.org/10.1785/0220160221>
- Chiodini, G. & Frondini, F. 2001. Carbon dioxide degassing from the Albani Hills volcanic region, Central Italy. *Chemical Geology*, **177**, 67–83, [https://doi.org/10.1016/S0009-2541\(00\)00382-X](https://doi.org/10.1016/S0009-2541(00)00382-X)
- Chiodini, G., Cioni, R., Guidi, M., Raco, B. & Narini, L. 1998. Soil CO₂ flux measurements in volcanic and geothermal areas. *Applied Geochemistry*, **13**, 543–552, [https://doi.org/10.1016/S0883-2927\(97\)00076-0](https://doi.org/10.1016/S0883-2927(97)00076-0)
- Chiodini, G., Frondini, F., Kerrick, D.M., Rogie, J., Parello, F., Peruzzi, L. & Zanzari, A.R. 1999. Quantification of deep CO₂ fluxes from Central Italy. Examples of carbon balance for regional aquifers and of soil diffuse degassing. *Chemical Geology*, **159**, 205–222, [https://doi.org/10.1016/S0009-2541\(99\)00030-3](https://doi.org/10.1016/S0009-2541(99)00030-3)
- Chiodini, G., Frondini, F., Cardellini, C., Parello, F. & Peruzzi, L. 2000. Rate of diffuse carbon dioxide Earth degassing estimated from carbon balance of regional aquifers: The case of central Apennine, Italy. *Journal of Geophysical Research*, **105**, 8423–8434, <https://doi.org/10.1029/1999JB900355>
- Chiodini, G., Avino, R. *et al.* 2004a. Fumarolic and diffuse soil degassing west of Mount Epomeo, Ischia, Italy. *Journal of Volcanology and Geothermal Research*, **133**, 291–309, [https://doi.org/10.1016/S0377-0273\(03\)00403-7](https://doi.org/10.1016/S0377-0273(03)00403-7)
- Chiodini, G., Cardellini, C., Amato, A., Boschi, E., Caliro, S., Frondini, F. & Ventura, G. 2004b. Carbon dioxide Earth degassing and seismogenesis in central and southern Italy. *Geophysical Research Letters*, **31**, L07615, <https://doi.org/10.1029/2004GL019480>
- Chiodini, G., Baldini, A., Carapezza, M., Cardellini, C., Frondini, F., Granieri, D. & Ranaldi, M. 2007. Carbon dioxide degassing at Lateral caldera (Italy): evidence of geothermal reservoir and evaluation of its potential energy. *Journal of Geophysical Research*, **112**, 2156–2202, <https://doi.org/10.1029/2006JB004896>
- Chiodini, G., Granieri, D., Avino, R., Caliro, S., Costa, A., Minopoli, G. & Vilardo, G. 2010. Non-volcanic CO₂ Earth degassing: Case of Mefite d'Ansanto (southern Apennines), Italy. *Geophysical Research Letters*, **37**, L11303, <https://doi.org/10.1029/2010GL042858>
- Chiodini, G., Caliro, S., Cardellini, C., Frondini, F., Inguaggiato, S. & Matteucci, F. 2011. Geochemical evidences for and characterization of CO₂ rich gas sources in the epicentral area of the Abruzzo 2009 earthquakes. *Earth and Planetary Science Letters*, **304**, 389–398, <https://doi.org/10.1016/j.epsl.2011.02.016>
- Chiodini, G., Cardellini, C., Caliro, S., Chiarabba, C. & Frondini, F. 2013. Advective heat transport associated with regional Earth degassing in central Apennine (Italy). *Earth and Planetary Science Letters*, **373**, 65–74.
- Civetta, L., Orsi, G., Scandone, P. & Pece, R. 1978. Eastwards migrations of the Tuscan anatectic magmatism due to anticlockwise rotation of the Apennines. *Nature*, **276**, 604–606.
- Civita, M. 1977. Osservazioni idrogeologiche nel versante sud occidentale del Massiccio del Cervati per la captazione delle sorgenti Fistole del Faraone. In: Nicotera, P. (ed.) *Memorie e note dell'Istituto di Geologia Applicata dell'Università di Napoli*, **13**, 5–36.
- Cosentino, D., Cipollari, P., Marsili, P. & Scrocca, D. 2010. Geology of the central Apennines: a regional review. *Journal of the Virtual Explorer*, **36**, paper 12, <https://doi.org/10.3809/jvirtex.2010.00223>
- Costa, A., Chiodini, G. *et al.* 2008. A shallow-layer model for heavy gas dispersion from natural sources: Application and hazard assessment at Caldara di Manziara, Italy. *Geochemistry, Geophysics, Geosystems*, **9**, Q03002, <https://doi.org/10.1029/2007GC001762>
- Della Vedova, B., Pellis, G., Foucher, J.P. & Rehault, J.P. 1984. Geothermal structure of Tyrrhenian Sea. *Marine Geology*, **55**, 271–289, [https://doi.org/10.1016/0025-3227\(84\)90072-0](https://doi.org/10.1016/0025-3227(84)90072-0)
- Di Luccio, F., Chiodini, G., Caliro, S., Cardellini, C., Convertito, V., Pino, N.A., Tolomei, C. & Ventura, G. 2018. Seismic signature of active intrusions in mountain chains. *Science Advances*, **4**, e1701825, <https://doi.org/10.1126/sciadv.1701825>
- Deutsch, C.V. & Journel, A.G. 1998. *GSLIB: Geostatistical Software Library and User's Guide*. Oxford University Press, New York.
- Evans, M.J., Derry, L.A. & France-Lanord, C. 2008. Degassing of metamorphic carbon dioxide from the Nepal Himalaya. *Geochemistry, Geophysics, Geosystems*, **9**, Q04021, <https://doi.org/10.1029/2007GC001796>
- Favara, R., Giammanco, S., Inguaggiato, S. & Pecoraino, G. 2001. Preliminary estimate of CO₂ output from Pantelleria Island volcano (Sicily, Italy): evidence of active mantle degassing. *Applied Geochemistry*, **16**, 883–894.
- Foley, S.F. 1992. Petrological characterization of the source components of potassic magmas: Geochemical and experimental constraints. *Lithos*, **28**, 187–204.
- Fresia, C. & Frezzotti, M.L. 2015. The dilemma of the dwarf Earth's CO₂ degassing: Irrelevant or crucial? *Journal of Geochemical Exploration*, **152**, 118–122, <https://doi.org/10.1016/j.gexplo.2015.02.006>
- Frezzotti, M.L., Peccerillo, A. & Panza, G. 2009. Carbonate metasomatism and CO₂ lithosphere–asthenosphere degassing beneath the Western Mediterranean: An integrated model arising from petrological and geophysical data. *Chemical Geology*, **262**, 108–120.
- Frondini, F., Chiodini, G., Caliro, S., Cardellini, C., Granieri, D. & Ventura, G. 2004. Diffuse CO₂ degassing at Vesuvio, Italy. *Bulletin of Volcanology*, **66**, 642–651, <https://doi.org/10.1007/s00445-004-0346-x>
- Frondini, F., Caliro, S., Cardellini, C., Chiodini, G., Morgantini, N. & Parello, F. 2008. Carbon dioxide degassing from Tuscany and Northern Latium (Italy). *Global and Planetary Change*, **61**, 89–102, <https://doi.org/10.1016/j.gloplacha.2007.08.009>
- Frondini, F., Cardellini, C., Caliro, S., Chiodini, G. & Morgantini, N. 2012. Regional groundwater flow and interactions with deep fluids in western Apennine: the case of Narni–Amelia chain (Central Italy). *Geofluids*, **12**, 182–196.
- Gaillardet, J. & Galy, A. 2008. Atmospheric science: Himalaya – carbon sink or source? *Science*, **320**, 1727–1728, <https://doi.org/10.1126/science.1159279>
- Gaillardet, J., Dupré, B., Louvat, P. & Allègre, C.J. 1999. Global silicate weathering and CO₂ consumption rates deduced from the chemistry of large rivers. *Chemical Geology*, **159**, 3–30, [https://doi.org/10.1016/S0009-2541\(99\)00031-5](https://doi.org/10.1016/S0009-2541(99)00031-5)
- Gambardella, B., Cardellini, C., Chiodini, G., Frondini, F., Marini, L., Ottonello, G. & Vetuschi Zuccolini, M. 2004. Fluxes of deep CO₂ in the volcanic areas of central–southern Italy. *Journal of Volcanology and Geothermal Research*, **136**, 31–52, <https://doi.org/10.1016/j.jvolgeores.2004.03.018>
- Girault, F., Koirala, B.P., Bhattarai, M. & Perrier, F. 2016. Radon and carbon dioxide around remote Himalayan thermal springs. In: Gillmore, G.K., Perrier, F.E. & Crockett, R.G.M. (eds) *Radon, Health and Natural Hazards*. Geological Society, London, Special Publications, **451**, 155–181, <https://doi.org/10.1144/SP451.6>
- Gorman, P.J. & Kerrick, D.M. 2006. Modeling open system metamorphic decarbonation of subducting slabs. *Geochemistry, Geophysics, Geosystems*, **7**, Q04007, <https://doi.org/10.1029/2005GC001125>
- Granieri, D., Chiodini, G., Avino, R. & Caliro, S. 2014. Carbon dioxide emission and heat release estimation for Pantelleria Island (Sicily, Italy). *Journal of Volcanology and Geothermal Research*, **275**, 22–23, <https://doi.org/10.1016/j.jvolgeores.2014.02.011>
- Hunt, J.A., Zafu, A., Mather, T.A., Pyle, D.M. & Barry, P.H. 2017. Spatially variable CO₂ degassing in the main Ethiopian Rift: implications for magma storage, volatile transport, and rift-related emissions. *Geochemistry, Geophysics, Geosystems*, **18**, <https://doi.org/10.1002/2017GC006975>
- Ingebritsen, S.E. & Mariner, R.H. 2010. Hydrothermal heat discharge in the Cascade Range, northwestern United States. *Journal of Volcanology and Geothermal Research*, **196**, 208–218.
- Ingebritsen, S.E., Sherrod, D.R. & Mariner, R.H. 1989. Heat-flow and hydrothermal circulation in the Cascade Range, north-central Oregon. *Science*, **243**, 1458–1462.
- Irwin, W.P. & Barnes, I. 1980. Tectonic relations of carbon dioxide discharges and earthquakes. *Journal of Geophysical Research*, **85**, 2156–2202, <https://doi.org/10.1029/JB085iB06p03115>
- Kerrick, D.M. 2001. Present and past non-anthropogenic CO₂ degassing from the solid earth. *Reviews of Geophysics*, **39**, 565–585, <https://doi.org/10.1029/2001RG000105>
- Kerrick, D.M. & Caldeira, K. 1993. Paleatmospheric consequences of CO₂ released during early Cenozoic regional metamorphism in the Tethyan orogen. *Chemical Geology*, **108**, 201–230, [https://doi.org/10.1016/0009-2541\(93\)90325-D](https://doi.org/10.1016/0009-2541(93)90325-D)

- Kerrick, D.M. & Caldeira, K. 1998. Metamorphic CO₂ degassing from orogenic belts. *Chemical Geology*, **145**, 2013–2232, [https://doi.org/10.1016/S0009-2541\(97\)00144-7](https://doi.org/10.1016/S0009-2541(97)00144-7)
- Kerrick, D.M., McKibben, M.A., Seward, T.M. & Caldeira, K. 1995. Convective hydrothermal CO₂ emission from high heat flow regions. *Chemical Geology*, **121**, 285–293, [https://doi.org/10.1016/0009-2541\(94\)00148-2](https://doi.org/10.1016/0009-2541(94)00148-2)
- Lee, H., Muirhead, J.D., Fischer, T.P., Ebinger, C.J., Kattenhorn, S.A., Sharp, Z.D. & Kianji, G. 2016. Massive and prolonged deep carbon emissions associated with continental rifting. *Nature Geoscience*, **9**, 145–149, <https://doi.org/10.1038/ngeo2622>
- Lucidi, B. 2010. *Caratterizzazione del degassamento di CO₂ nel sistema di Torre Alfina (VT)*. Masters thesis, Università degli Studi di Perugia, Perugia.
- Manga, M. 1998. Advective heat transport by low-temperature discharge in the Oregon Cascades. *Geology*, **26**, 799–802.
- Manga, M. & Kirchner, J.W. 2004. Interpreting the temperature of water at cold springs and the importance of gravitational potential energy. *Water Resources Research*, **40**, W05110.
- Marty, B. & Tolstikhin, I.N. 1998. CO₂ fluxes from mid-ocean ridges, arcs and plumes. *Chemical Geology*, **145**, 233–248, [https://doi.org/10.1016/S0009-2541\(97\)00145-9](https://doi.org/10.1016/S0009-2541(97)00145-9)
- Minissale, A. 2004. Origin, transport and discharge of CO₂ in central Italy. *Earth-Science Reviews*, **66**, 89–141, <https://doi.org/10.1016/j.earscirev.2003.09.001>
- Mörner, N.A. & Etiope, G. 2002. Carbon degassing from the lithosphere. *Global and Planetary Change*, **33**, 185–203, [https://doi.org/10.1016/S0921-8181\(02\)00070-X](https://doi.org/10.1016/S0921-8181(02)00070-X)
- Parkhurst, D.L. & Appelo, C.A.J. 1999. *User guide to PHREEQC (Version 2) – a computer program for speciation, batch-reaction, one-dimensional transport, and inverse geochemical calculations*. US Geological Survey, Water Resources Investigation Report, **99-4259**.
- Peccerillo, A. 1999. Multiple mantle metasomatism in central-southern Italy: Geochemical effects, timing and geodynamic implications. *Geology*, **27**, 315–318.
- Peccerillo, A. & Frezzotti, M.L. 2015. Magmatism, mantle evolution and geodynamics at the converging plate margins of Italy. *Journal of the Geological Society, London*, **172**, 407–427, <https://doi.org/10.1144/jgs2014-085>
- Pecoraino, G., Brusca, L., D'Alessandro, W., Giammanco, S., Ingauggiato, S. & Longo, M. 2005. Total CO₂ output from Ischia Island volcano (Italy). *Geochemical Journal*, **39**, 451–458.
- Rapa, G., Groppo, C., Rolfo, F., Petrelli, M., Mosca, P. & Perugini, D. 2017. Titanite-bearing calc-silicate rocks constrain timing, duration and magnitude of metamorphic CO₂ degassing in the Himalayan belt. *Lithos*, **292–293**, 364–378, <https://doi.org/10.1016/j.lithos.2017.09.02>
- Rogie, J.D., Kerrick, D.M., Chiodini, G. & Frondini, F. 2000. Flux measurements of nonvolcanic CO₂ emission from some vents in central Italy. *Journal of Geophysical Research*, **105**, 8435–8445, <https://doi.org/10.1029/1999JB900430>
- Rose, T.P. & Davison, M.L. 1996. Radiocarbon in hydrologic systems containing dissolved magmatic carbon dioxide. *Science*, **273**, 1367–1370, <https://doi.org/10.1126/science.273.5280.1367>
- Seward, T.M. & Kerrick, D.M. 1996. Hydrothermal CO₂ emission from the Taupo Volcanic Zone, New Zealand. *Earth and Planetary Science Letters*, **139**, 105–113, [https://doi.org/10.1016/0012-821X\(96\)00011-8](https://doi.org/10.1016/0012-821X(96)00011-8)
- Sorey, M.L., Evans, W.C., Kennedy, B.M., Farrar, C.D., Hainsworth, L.J. & Hausback, B. 1998. Carbon dioxide and helium emissions from a reservoir of magmatic gas beneath Mammoth Mountain, California. *Journal of Geophysical Research: Solid Earth*, **103**, 15503–15323, <https://doi.org/10.1029/98JB01389>
- Walker, J.C.G., Hays, P.B. & Kasting, J.F. 1981. A negative feedback mechanism for the long-term stabilization of Earth's surface temperature. *Journal of Geophysical Research*, **86**, 9776–9782, <https://doi.org/10.1029/JC086iC10p09776>
- Wigley, T.M.L., Plummer, N.L. & Pearson, F.J., Jr. 1978. Mass transfer and carbon isotope evolution in natural water systems. *Geochimica et Cosmochimica Acta*, **42**, 1117–1139, [https://doi.org/10.1016/0016-7037\(78\)90108-4](https://doi.org/10.1016/0016-7037(78)90108-4)